

EMCal Barrel Optimization for SiD Note

Performance of Alternate Layering Schemes

Da An^{†,‡}, M. Breidenbach[†], N. Graf[†], and J. McCormick[†]

[†]*SLAC National Accelerator Laboratory*

[‡]*California Institute of Technology*

(Dated: September 23, 2014)

1 Introduction

In this study, our main goal is to simultaneously optimize EMCal cost and performance. Currently, the estimated EMCal cost is upwards of \$100 million. A large portion ($\sim 50\%$) of the cost originates from the multiple layers of silicon detectors, each layer costing \sim \$2 million. This motivates us to focus our study on different layering schemes and their impact with regards to EMCal performance.

We start off with Section 2, which provides an overview of the detector specifications used for this analysis. Before we dive into the main results, some peculiar findings in the EMCal calibration steps are noted in Section 3. We then go on to quantify the performance of alternate EMCals with several measures. In Section 4, a look into the performance of single photon events for our alternate EMCals is presented. In Section 5, we look at events with two photons. Section 6 provides a performance analysis for how PandoraPFA works with up quark jets. Finally, we summarize and discuss the pertinent results in Section 7.

2 Alternate EMCals

The current EMCal scheme is part of the sidloi3 detector, and is composed of 30 (20+10) layers, where each of the first 20 layers consist of 2.5 mm Tungsten, 0.32 mm Silicon, 0.05 mm Copper, and 0.30 mm Kapton, and the latter 10 layers have the same specifications with a different Tungsten thickness of 5.0 mm. A quarter cross sectional images of the sidloi3 EMCal can be seen in Fig. 7.

For consistency in the scope of the whole detector geometry, we constrain all the alternate EMCal designs to have a fixed total Tungsten thickness of 100 mm, so only the number of silicon layers is changed; this prevents overlaps and gaps among the Tracker, EMCal, and HCal. We look at 10 alternate EMCal designs and study their performance with photons and light quark jets. The specifications of these 10 designs can be found in Tables 1 (Group 1), 2 (Group 2), 3 (Group 3). These designs were chosen in order to study a broad range of possibilities and effects. We do not go below 2.5 mm of Tungsten thickness because it is the thinnest mechanically sound. Note that we only change the layering schemes of the EMCal Barrel. Because of this, we keep our study limited to events purely in the EMCal Barrel.

Tungsten thicknesses for EMCals with fixed 2.5 mm thin layers				
Layer Count	15	20	25	30*
Thin+Thick Count	10+5	13+7	17+8	20+10
Individual Thins (mm)	2.5	2.5	2.5	2.5
Individual Thicks (mm)	15.0	9.64	7.18	5.0
Total Thins (mm)	25.0	32.5	42.5	50.0
Total Thicks (mm)	75.0	67.5	57.5	50.0

Table 1: Specifications for alternate EMCal designs with the thin layers held fixed at 2.5 mm thickness per layer. For ease of reference, we collectively call these alternate EMCal designs “Group 1”. ***Bold face indicates the current sidloi3 detector.**

Tungsten thicknesses for EMCals with fixed total thins to total thicks ratio				
Layer Count	15	20	25	30*
Thin+Thick Count	10+5	13+7	17+8	20+10
Individual Thins (mm)	5.0	3.84	2.90	2.5
Individual Thicks (mm)	10.0	7.14	6.25	5.0
Total Thins (mm)	50.0	50.0	50.0	50.0
Total Thicks (mm)	50.0	50.0	50.0	50.0

Table 2: Specifications for alternate EMCAL designs with the ratio of total thin layer to total thick layer thickness held fixed at 1:1 (50mm : 50mm). For ease of reference, we collectively call these alternate EMCAL designs “Group 2”. ***Bold face indicates the current sidloi3 detector.**

Tungsten thicknesses for EMCals with varying thin to thick layer ratio				
Layer Count	25	25	30	30
Thin+Thick Count	15+10	20+5	15+15	25+5
Individual Thins (mm)	2.5	2.5	2.5	2.5
Individual Thicks (mm)	6.25	10.0	4.16	7.5
Total Thins (mm)	37.5	50.0	37.5	62.5
Total Thicks (mm)	62.5	50.0	62.5	37.5
Thin : Thick Ratio	3:2	4:1	1:1	5:1

Table 3: Specifications for alternate EMCAL designs with varying layer count ratios; note that the current sidloi3 design has a 2:1 ratio. For ease of reference, we collectively call these alternate EMCAL designs “Group 3”.

3 Calibration

Currently, the EMCAL is calibrated with single photons fired at $\theta = 90^\circ$ and $\phi = 0^\circ$. These photon events deposit raw energy into the thin EMCAL layers, thick EMCAL layers, and Hcal layers. We then solve for the sampling fractions for each of the three different layers types based upon the MC energy of the photons. There is no angular dependence within the sampling fractions, meaning that the calibration is only “perfect” for photons at $\theta = 90^\circ$ and $\phi = 0^\circ + n \cdot 30^\circ$. For the discussion in this section, we deal with only the current sidloi3 design.

3.1 θ Dependence

The effect of θ angle on the reconstructed energy and resolution of a single photon is small but real. We study only 10 GeV photons with angles ranging from the center of the EMCAL Barrel ($\theta = 90^\circ$) to the edge ($\theta = 140^\circ$). The resolution remains relatively constant. However, there is a $\sim 1\%$ reconstructed energy difference from the center to the edge. We expect the reconstructed energy to decrease as θ increases since the photons pass through more absorber, which means it should deposit less raw energy into the detector. However, we see an increase in reconstructed energy as θ increases, which goes against our intuition. This effect can be seen in Fig. 1.

3.2 ϕ Dependence

The ϕ angle dependence is an effect intrinsic of the EMCAL layout. The current EMCAL consists of twelve overlapping trapezoidal staves which give it an overall dodecagon cross section. The ϕ angles at which the staves overlap is where the problem arises. In these regions, there are not exactly 20 thin layers and 10 thick layers. In fact, a photon traveling . As a result, the reconstructed energy distribution of the photon is skewed. For example, a photon at $\phi = 15^\circ$ will pass through only thin layers, so we should use the thin layer sampling fraction for all the hits. However, the current reconstruction algorithm uses the 20 thin plus 10 thick layer sampling fraction scheme. In this scenario, the reconstructed energy is larger than the MC energy. This effect also contributes to a degraded energy resolution, which can be seen from the fits in Fig. 2.

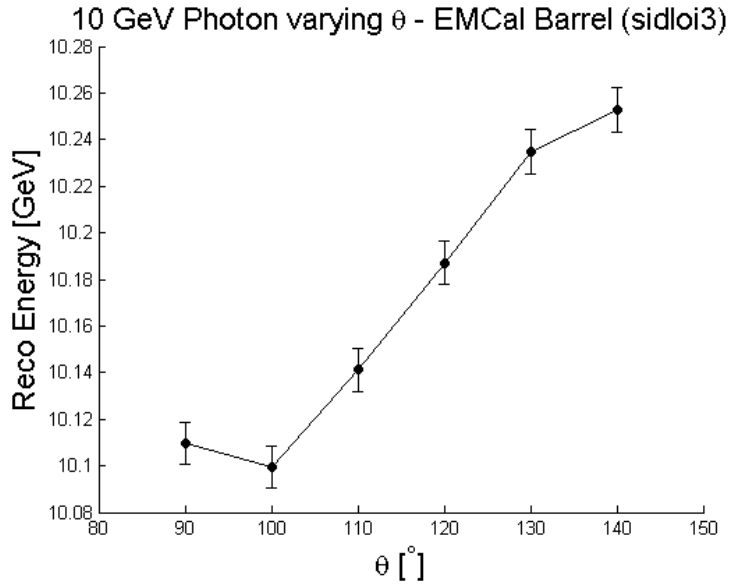


Figure 1: Reconstructed energy of a 10 GeV photon as a function of the θ angle at which the photon was fired. This is for the sidloi3 detector.

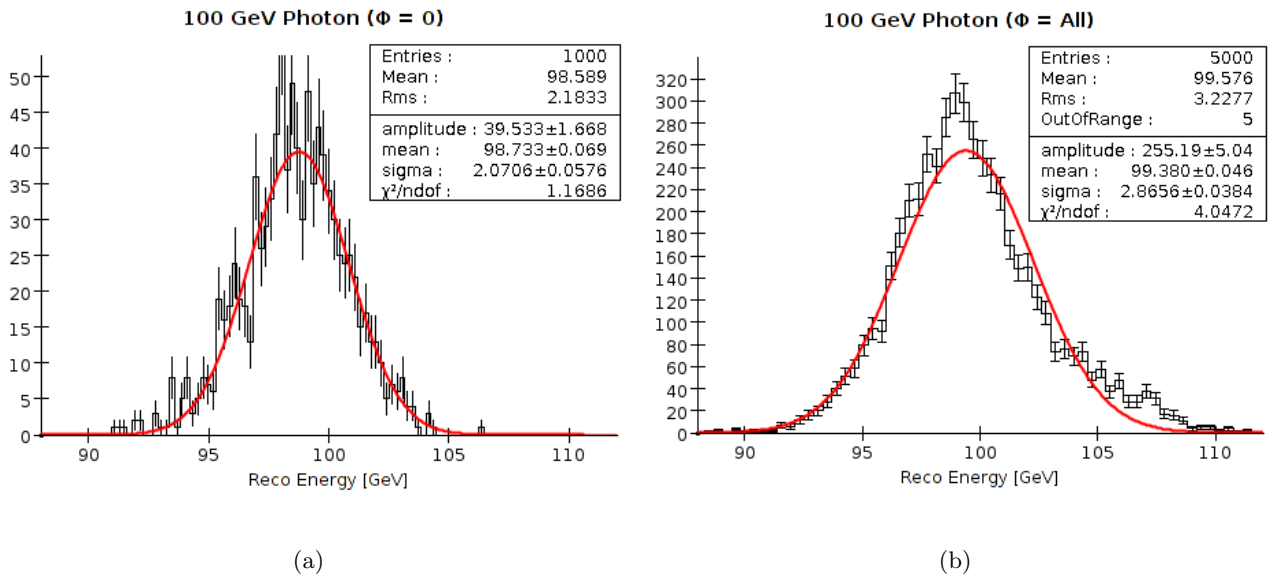


Figure 2: Comparison of the energy distribution of 100 GeV photons with (a) $\phi = 0$ and (b) $\phi = \text{all}$. Note that in (b), there is an excess at higher energies, which contributes to a worsening in resolution.

4 Single Photon Study

This section focuses on the reconstructed energy resolution of single photon events as a measure of the performance of alternate detectors. We define resolution as σ_E/\sqrt{E} , where σ_E , E , and their error are given from a Gaussian fit. The single photon samples are simulated with SLIC, a Geant4 application. There are 1000 events for each MC energy, and all photons are fired from the origin at $\theta = 90^\circ$ and $\phi = 0^\circ$. In the following data results, there are two aspects that signify how well the resolutions are. The first is the obvious measure of the mean $\%/\sqrt{E}$ resolution, The second is the range of $\%/\sqrt{E}$ for varying energies. In a uniform sampling calorimeter, the range is nominally zero. Our alternate EMCals are composed of two different thickness absorbers, so we see a range of resolutions for varying photon energies since higher energy photons penetrate deeper into the EMCal and interact more with the thick absorbers. This resolution range reinforces our expectation that thinner absorbers give better resolution than thicker ones. A summary of the results can be seen in Fig. 3. More detailed plots for each Group can be seen in Fig. 8.

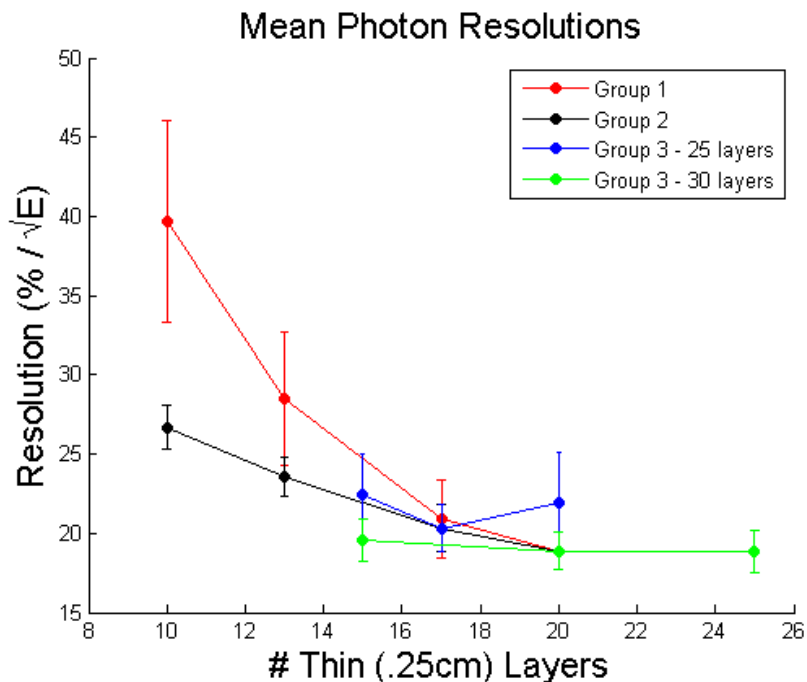


Figure 3: The mean photon resolutions of each alternate EMCal design, where the mean is calculated by averaging photons with MC energies of 1, 2, 5, 10, 20, 50, and 100 GeV; the error bars are the standard deviations of those data points, and they directly reflect the range of the data points.

[Group 1]: In this set of alternate EMCals, the mean resolution degrades by only 1 – 3% when going from 30 layers to 25 layers. As we venture to smaller layer counts of 20 and 15, the resolution significantly worsens to the point that there is no reason to suspect good resolution with less than 20 layers of silicon detectors. Also, the resolution range increases drastically as we lower the layer count.

[Group 2]: In terms of mean $\%/\sqrt{E}$, we see the same behavior in Group 2 as in Group 1. The difference is that Group 2 exhibits a smaller resolution range than Group 1. In fact, the range between 2 GeV and 50 GeV photons remains fairly constant for all layering schemes. A comparison with Group 1 suggests that the range is minimum when the ratio of the total thicknesses of the thin and thick layers is close to 1 (50 mm/50 mm in this case).

[Group 3]: This group of alternate EMCals was created to study varying ratios of thin to thick layer counts for a given total layer count. From Fig. 3, we see that the mean resolution for the 25 layer and 30 layer schemes remains constant, but the range changes such that schemes with ratios near 1 exhibit smaller ranges. Note that this statement is independent of the range differences shown in Groups 1 and 2.

5 $\pi^0 \rightarrow \gamma\gamma$

5.1 Energy Resolution

Here, we look at the π^0 decay in order to better understand the performance of the reconstruction algorithm (PandoraPFA) with various EMCal designs. The π^0 samples are simulated with slicPandora with 2500 events for each MC energy ranging from 1 GeV to 100 GeV. Since the final state particles of the π^0 are photons, we expect to see the same behavior in resolution for the π^0 samples as we saw with the single photons. A summary of the π^0 resolutions are shown in Fig. 4. From this plot, we see that the π^0 's do behave similarly to single photons.

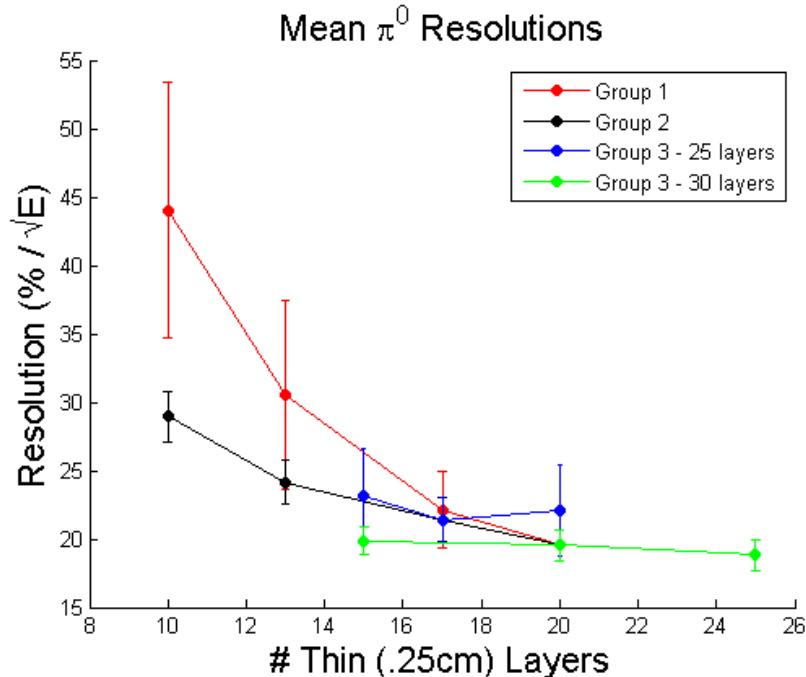


Figure 4: The mean π^0 resolutions of each alternate EMCal design, where the mean is calculated by averaging π^0 's with MC energies of 1, 2, 5, 10, 20, 50, and 100 GeV; the error bars are the standard deviations of those data points, and they directly reflect the range of the data points.

5.2 Distinguishing Photons

Knowing that our π^0 samples are acceptable, we go on to characterize how well the PandoraPFA algorithm can distinguish the two photons in a π^0 decay. Scanning over π^0 energies is analogous to scanning over diphoton separation angles since the separation angle, α , between two photons decayed from a π^0 is roughly given by

$$\alpha \sim \arcsin\left(\frac{m_\pi}{E_\pi}\right)$$

We expect that as the π^0 energy increases, i.e. as separation angle gets smaller, the algorithm will reconstruct the two photons into one. The limiting cases should be 2 reconstructed photons at low energy and 1 reconstructed photon at high energy. This behavior can be seen in Fig. 5. The limiting cases in this plot are off from what we expect because of the minimum energy cuts within PandoraPFA. With more sophisticated cuts and input parameters, the limiting cases should converge to 2 and 1 reconstructed photon(s). The main thing to note from Fig. 5 is that PandoraPFA performs similarly for all detector variants from Groups 1 and 2. This result suggests that the reconstruction algorithm is dependent mostly upon the lateral distribution of the pixels within each Silicon detector layer (which we keep the same for all alternate EMCals) rather than the layering scheme of the Tungsten absorbers and Silicon detectors.

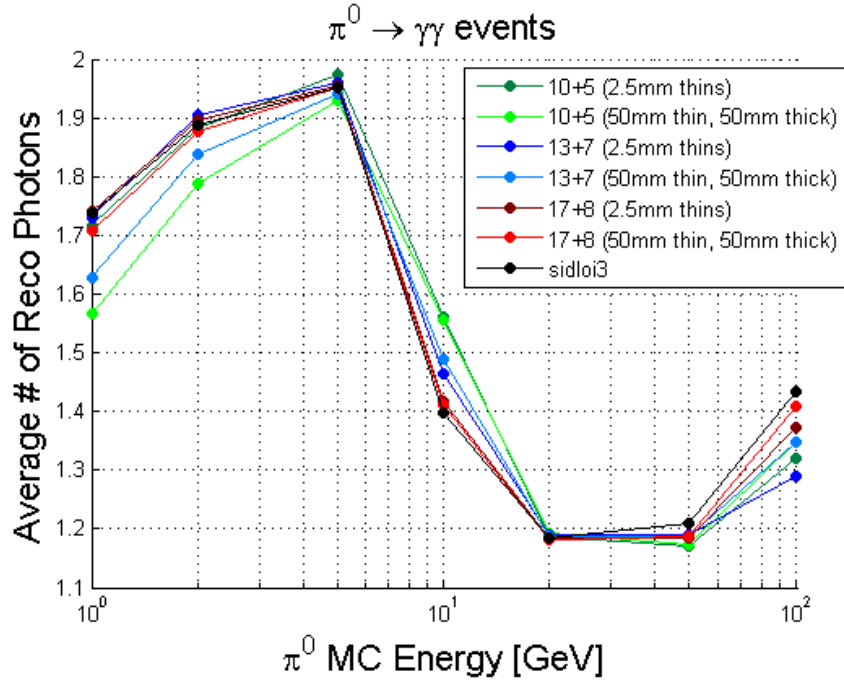


Figure 5: Plot of how well PandoraPFA can distinguish between two photons, whose separation angle is controlled by the energy of the π^0 . Lower energies correspond to large angle and higher energies correspond to small angle.

6 up quark jets

This section focuses on the reconstructed energy resolution of up quark jets as a measure of the performance of our various detector designs. It is similar to the single photon study in Section 4, but the main difference is that we now define resolution as σ_E/E rather than σ_E/\sqrt{E} , where σ_E , E , and their

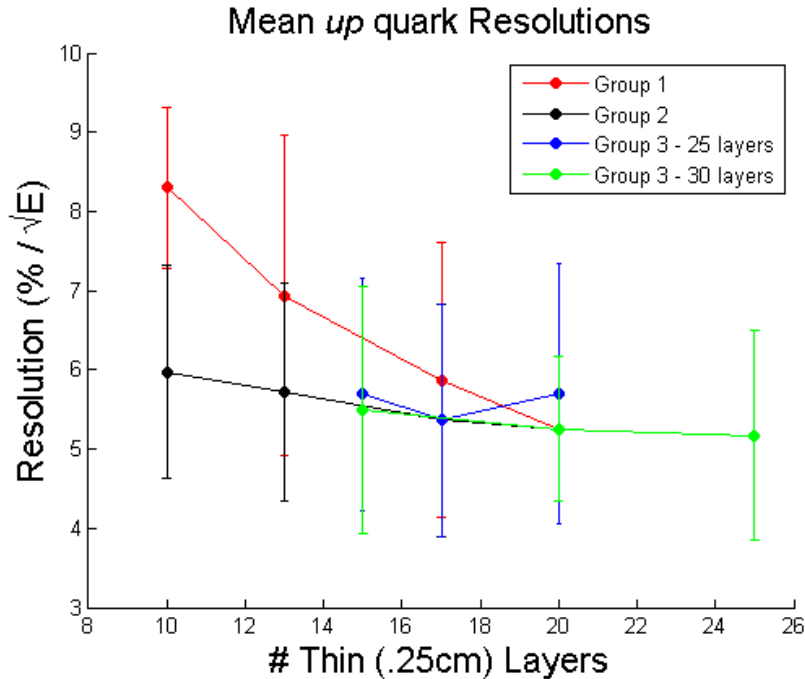


Figure 6: The mean up quark resolutions of each alternate EMCAL design, where the mean is calculated by averaging π^0 's with MC energies of 50, 100, 250, and 500 GeV; the error bars are the standard deviations of those data points, and they directly reflect the range of the data points.

error are given by a Gaussian fit. The up quarks are simulated using slicPandora with 10,000 events for each MC energy. The up quarks are fired at all angles, but we only take those events that are detected solely within the EMCal Barrel.

The results are summarized in Fig. 6, and more detailed plots of the resolutions can be seen in Fig. 11. The trends in the results are rather similar to the single photon and π^0 studies, so please refer to Section 4 for a more detailed explanation of the results. The only slight difference is that the resolution ranges of the up quarks remain relatively constant for all EMCal designs. An example fit of a 500 GeV up quark can be found in Fig. 10. Notice that the mean of the fit is offset from the MC energy. This effects our resolution since σ_E/E is calculated with the fitted E rather than the MC E .

7 Conclusion

Here, we will note a few of the important points of this study. (1) There are small but real issues with the calibration and better precision may be achieved if angular dependencies are included in the calibration of the EMCal. (2) With regards to resolution, the performance of EMCals with layers between 25 and 30 is good enough that they may be considered as possible alternatives to the current sidloi3; any layer count lower than 25 seems unreasonable. (3) With regards to resolution range, any future modifications to the EMCal should aim for two factors in order to minimize the range - keep the ratio of [# thin layers] : [# thick layers] close to 1:1 and keep the ratio of [total thickness of thin layers] : [total thickness of thick layers] close to 1:1. (4) It seems that the PandoraPFA reconstruction algorithm is dependent mostly upon the lateral distribution of the pixels within each Silicon detector layer (which we keep the same for all alternate EMCals) rather than the layering scheme of the Tungsten absorbers and Silicon detectors.

8 Acknowledgements

There are many people that I would like to acknowledge for making this summer a memorable and productive one. First off, thanks to Martin Breidenbach for this amazing opportunity at SLAC and for his great mentorship and guidance. Thanks to Norman Graf for his help with software and analysis code throughout the entire summer. Thanks to Jeremy McCormick for all his help in setting up the software systems for this study and ongoing software support. Also, thanks to Jan Strube and Marcel Stanitzki, and Christopher Sund for all their suggestions and help.

9 Figures

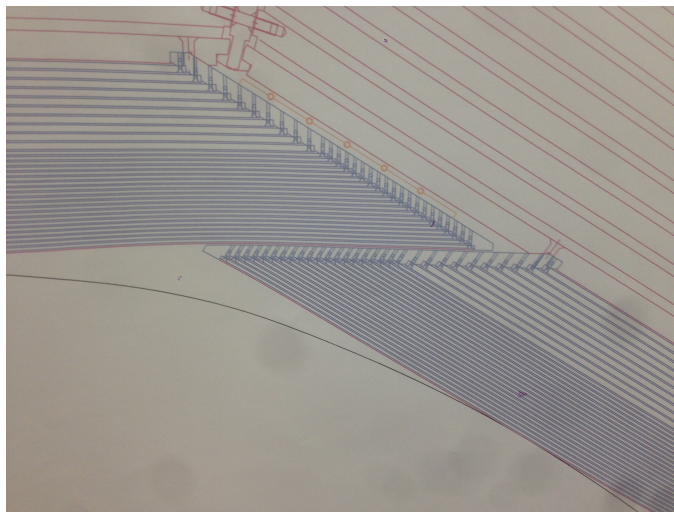
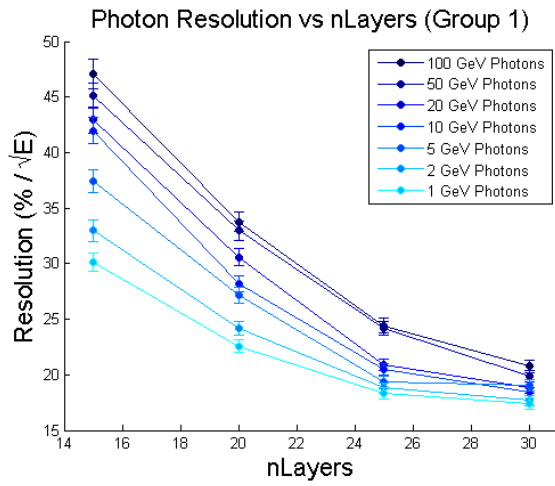
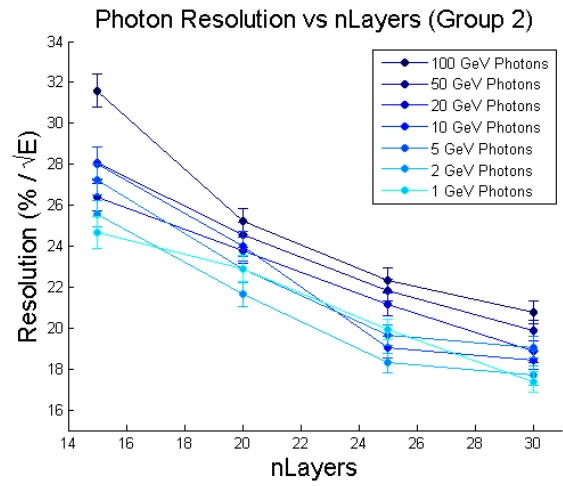


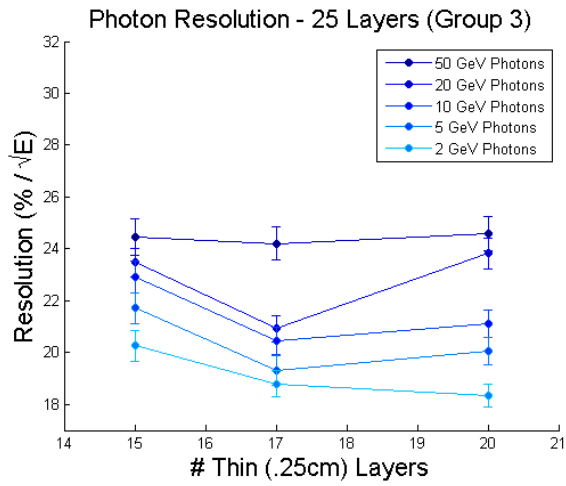
Figure 7: Cross sectional image of the current sidloi3 EMCal (shown in blue). Note the thin and thick layering scheme as well as the overlapping staves.



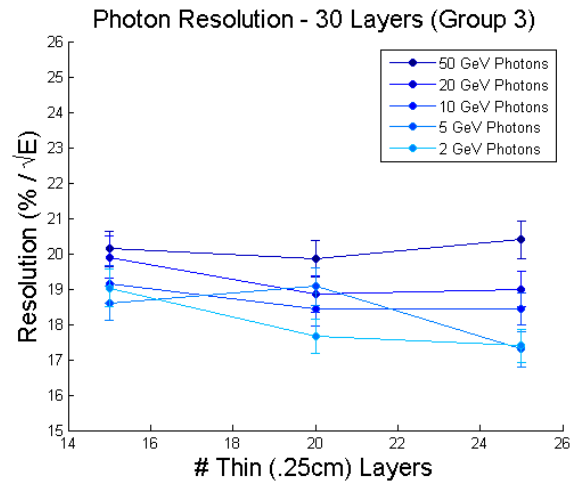
(a)



(b)



(c)



(d)

Figure 8: Resolutions of photons for all MC energies and alternate EMCAL designs.

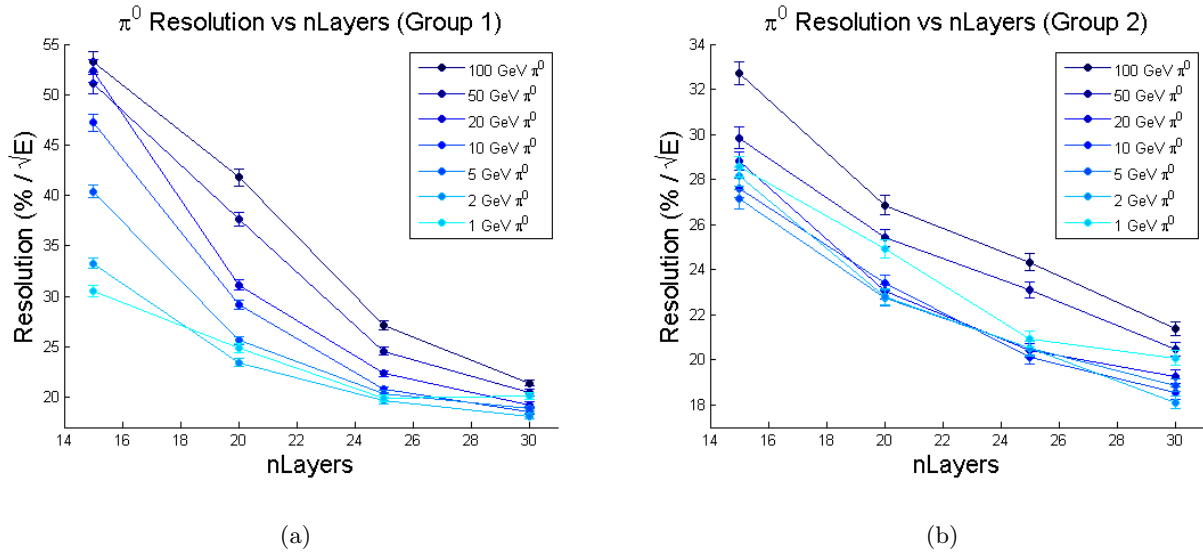


Figure 9: Resolutions of π^0 's for all MC energies and alternate EMCAL designs.

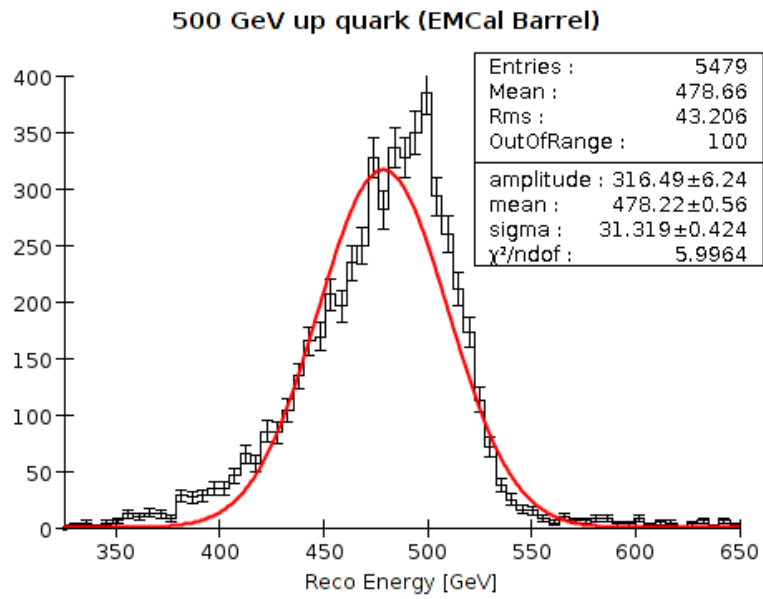
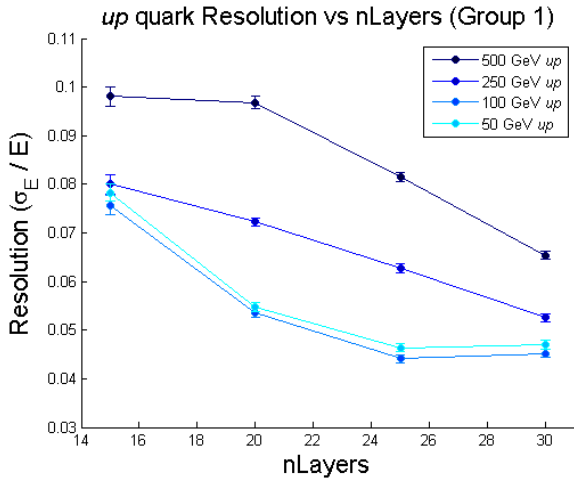
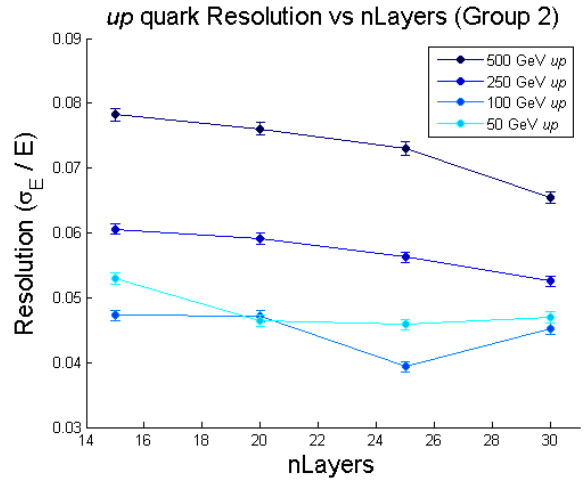


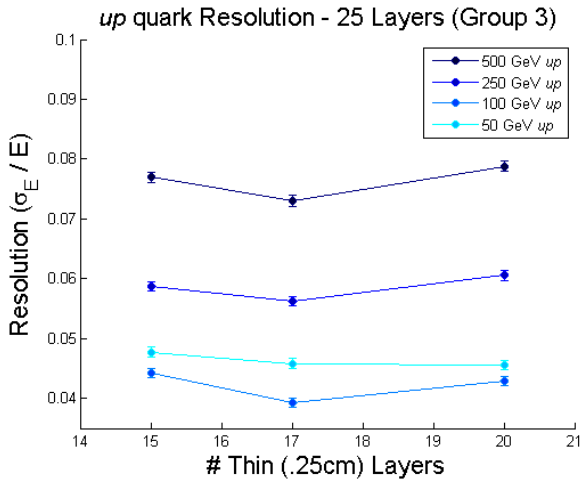
Figure 10: Example energy distribution and fit for a 500 GeV up quark for the sidloi3. Notice the offset of the fit from the MC energy. If I had more time, I'd try to make the fit better by using a different fit distribution or making more cuts on the up quark events.



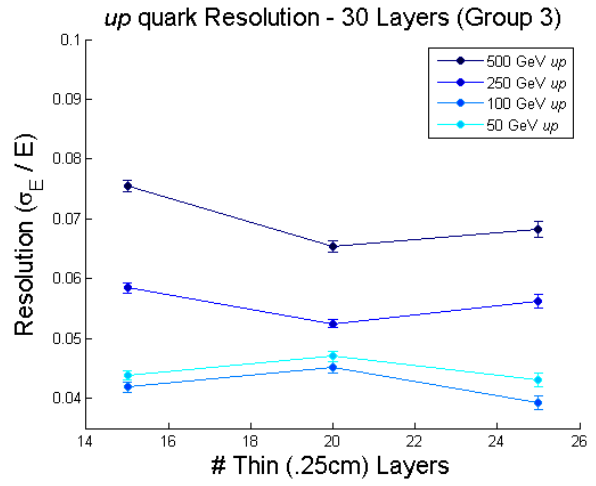
(a)



(b)



(c)



(d)

Figure 11: Resolutions of up quarks for all MC energies and alternate EMCAL designs.